

26 carbon (62-71%), total nitrogen (82-85%) and total phosphorous (90-92%). Finally, Zn-
27 REs accounted for 26% in R3, 37% in R2, and 49% in R1 and R4.

28

29 **Keywords:** Algal-bacterial processes; biomass production; heavy metal removal;
30 microalgae dynamics; piggery wastewater treatment.

31

32 **1. Introduction**

33 The current global energy and climate change crisis has triggered the quest for
34 alternative green energy sources with a low carbon dioxide (CO₂) footprint (González-
35 Fernández et al., 2012a). In this context, microalgae have emerged as a promising
36 renewable energy platform due to their ability to transform sunlight directly into gas
37 biofuels (i.e H₂) or an organic biomass feedstock that can be further bioconverted into
38 multiple liquid and gas biofuels (Richmond, 2004). Thus, microalgal biomass can be
39 anaerobically digested yielding biogas (CH₄ + CO₂) and a nutrient rich digestate
40 (Ehimen et al., 2011; González-Fernández et al., 2012b). In addition, while the lipid
41 fraction of microalgae can be transesterified into biodiesel (Vimalarasan et al., 2011),
42 the carbohydrate fraction can be fermented into bioethanol (Naik et al., 2010) or
43 biohydrogen (Chandrasekhar et al., 2015). Microalgae exhibit multiple advantages over
44 conventional energy crops such as high areal productivities (50-100 tn/ha·y), cultivation
45 in non-arable land (preventing competition with food) and high lipid or carbohydrate
46 fractions depending on the cultivation conditions. Likewise, microalgae can be
47 cultivated in fresh, marine or wastewaters (Cheah et al., 2016).

48

49 In this context, nutrient-rich wastewaters represent a valuable feedstock to reduce the
50 costs of microalgae and cyanobacteria (from now on referred to as microalgae)

51 cultivation, which will ultimately increase the cost-competitiveness of microalgae-based
52 biofuels (Acién et al., 2016). Algal-bacterial symbiosis can combine a low-cost mass
53 production of biomass with the treatment of wastewater to levels required for discharge
54 into natural water bodies. Indeed, both domestic, industrial and livestock wastewaters
55 have successfully supported microalgae cultivation (Muñoz et al., 2003; Muñoz and
56 Guieysse, 2006). During microalgae-based wastewater treatment, both the organic
57 carbon, nitrogen and phosphorous present in the residual effluent are assimilated into
58 algal-bacterial biomass. Heavy metals and pathogens are also efficiently removed
59 during microalgae growth as a result of adsorption and pH-mediated mechanisms.
60 Despite microalgae cultivation in wastewater entails significant economic and
61 environmental advantages over axenic mass production of microalgae in mineral salt
62 media, controversy still exists in literature about the possibility of maintaining
63 monoalgal cultures with a constant biomass composition during microalgae-based
64 wastewater treatment. This is central to the development of microalgae-based
65 biorefineries for biofuel production, whose viability depends on the supply of a biomass
66 with a consistent year-round composition and characteristics. Hence, while most studies
67 conducted under laboratory or outdoors conditions focused on the removal of key
68 pollutants present in wastewater, little attention has been paid to the monitoring of the
69 dynamics of microalgae population.

70

71 Pig production is a key economic sector in many countries in Europe, accounting for
72 148.7 million pigs heads and 44.3% of the total European livestock (EU, 2015;
73 MAGRAMA, 2015) in 2015. European pig farming generates 217- 434 million m³/y (4-
74 8 L/day/pig) of piggery wastewater containing high concentrations of organic matter
75 and nutrients (De Godos et al., 2009). The estimated average organic matter and nutrient

76 load present in EU piggery wastewaters in 2015 amounted to 8.923.000 tn chemical
77 oxygen demand (COD)/y, 890.000 tn nitrogen (N)/y and 223.000 tn phosphorous (P)/y
78 (EU, 2016). In addition, piggery wastewater can contain high concentrations of heavy
79 metals such as Zinc and Copper, typically used as growth promoters in swine nutrition
80 (Abe et al., 2012; De la Torre et al., 2000).

81

82 The experimental work herein conducted evaluated the dynamics of microalgae
83 population during piggery wastewater treatment in four open continuous
84 photobioreactors inoculated with two green microalgae species, a cyanophyta, and
85 without inoculum. In addition, the influence of the microalgae inoculum on the steady
86 state organic matter, nutrient and heavy metal removal was assessed.

87

88 **2. Materials and methods**

89 **2.1. Microalgae**

90 *Chlorella minutissima* Fott and Nováková was obtained from an indoor high rate algal
91 pond (HRAP) treating centrate at the Dept. of Chemical Engineering and Environmental
92 Technology from Valladolid University (Spain). *Acutodesmus obliquus* and *Oscillatoria*
93 *sp* were kindly provided by the Department of Chemical Engineering from Almeria
94 University (Spain).

95

96 **2.2. Piggery wastewater**

97 Fresh centrifuged piggery wastewater (PWW) was collected at a nearby farm at
98 Cantalejo (Spain) and stored at 4°C. The average composition of the piggery wastewater
99 diluted at 15% was: 1340±34 mg/L of total suspended solids (TSS), 1375±121 mg/L of

100 total organic carbon (TOC), 314±55 mg/L of inorganic carbon (IC), 393±26 mg/L of
101 total nitrogen (TN), 9.4±0.4 mg/L of total phosphorus (TP) and 0.7±0.2 mg/L of zinc
102 (Zn). Nitrate (NO₃⁻), nitrite (NO₂⁻), copper (Cu) and arsenic (As) concentrations
103 remained below detection limit (Table 1).

104

105 <Table 1>

106

107 **2.3. Experimental set-up**

108 The experimental set-up consisted of four 15.8 cm deep 3 L open photobioreactors
109 illuminated at 2800 μmol/m²·s for 12 hours a day (08h00 to 20h00) by LED lamps
110 arranged in a horizontal configuration 20 cm above the photobioreactor surface
111 (Figure1). The photobioreactors were immersed in a water bath to prevent the high
112 temperatures imposed by the LEDs irradiation. Immersion water pumps were used to
113 mix the algal-bacterial cultivation broth in the reactors. The photobioreactors were fed
114 with piggy wastewater diluted at 15% using an auto control 205U7CA multi-channel
115 cassette pump (Watson-Marlow, UK). The pH in the cultivation broth was
116 automatically maintained at 8.0 via CO₂ addition (CARBUROS METALICOS-
117 Barcelona, Spain) using a Crison multimeter M44 control unit (Crison Instruments,
118 Spain).

119

120 < Figure 1 >

121

122 **2.4. Experimental design**

123 Photobioreactors 1, 2 and 3 (namely R1, R2 and R3, respectively) were inoculated with
124 *Chlorella minutissima* Fott and Nováková, *Acutodesmus obliquus* and *Oscillatoria* sp.,
125 respectively, at an initial TSS concentration of 220 mg/L (corresponding to initial cell
126 concentrations of 1.750, 0.295 and $0.332 \cdot 10^9$ cells/L, respectively). Photobioreactor 4
127 (R4) was not inoculated and served as control. The photobioreactors, which were
128 initially filled with tap water, were operated at a hydraulic retention time (HRT) of ≈ 27
129 days (estimated based on the influent PWW) for 176 days. Photobioreactors effluents
130 overflowed separately as a function of the evaporation rates. Liquid samples of 30 mL
131 were weekly drawn from the influent PWW and effluent of R1, R2, R3 and R4 to
132 determine the concentrations of TOC, IC, TN, NO_2^- , NO_3^- , TP and TSS. Effluent
133 samples were filtered through 1 μm glass fiber filters prior analysis. Likewise, the
134 microalgae population structure in R1, R2, R3 and R4 was weekly assessed from
135 biomass samples preserved with lugol acid at 5% and formaldehyde at 10%, and stored
136 at 4 °C prior to analysis (only 8 samples from each photobioreactor were analyzed). The
137 dissolved oxygen and temperature of the cultivation broths were measured twice per
138 day, while the influent and effluent flowrates were daily recorded in all
139 photobioreactors to monitor water evaporation losses. Finally, the C, N and P content of
140 the algal bacterial biomass was measured under steady state at the end of the
141 experiment.

142

143 The C, N and P removal efficiencies (RE) were calculated according to Eq. (1):

$$144 \quad RE(\%) = \frac{(C_{feed} \times Q_{feed}) - (C_{eff} \times Q_{eff})}{C_{feed} \times Q_{feed}} \times 100 \quad (1)$$

145 where C_{feed} and C_{eff} represent the dissolved concentrations of TOC, IC, TN, TP and Zn
146 in the PWW and photobioreactors effluents, respectively, while Q_{feed} and Q_{eff} represent

147 the PWW and effluent flow rates. The process was considered under steady state when
148 the TSS concentrations in the photobioreactors remained stable for at least four
149 consecutive samplings (~ 1 month). The results were here provided as the average \pm
150 standard deviation from duplicate measurements along one month of steady state (days
151 150-176).

152

153 *2.5 Analytical procedures*

154 A Crison M44 multimeter and a Crison PH 28 meter were used for the on-line
155 measurement of the pH. Dissolved oxygen (DO) and temperature (T) were recorded
156 using an OXI 330*i* oximeter (WTW, Germany). A LI-250A light meter (LI-COR
157 Biosciences, Germany) was used to measure the light intensity as photosynthetically
158 active radiation (PAR). TOC, IC and TN concentrations were determined using a TOC-
159 V CSH analyzer equipped with a TNM-1 module (Shimadzu, Japan). Nitrate and nitrite
160 were analyzed by high performance liquid chromatography-ion conductivity (HPLC-IC)
161 in a Waters 515 HPLC pump coupled with a Waters 432 ionic conductivity detector and
162 equipped with an IC-Pak Anion HC (150 mm \times 4.6 mm) column. TSS and TP
163 concentrations were determined according to Standard Methods (APHA, 2005). The
164 analysis of the C, N and P content in the algal-bacterial biomass was carried out using a
165 LECO CHNS-932 elemental analyzer with pre-dried and grinded algal-bacterial
166 biomass. The concentration of Zn, Cu and As was determined using a 725-ICP Optical
167 Emission Spectrophotometer (Agilent, USA) at 213.62. The identification and
168 quantification of microalgae were conducted by microscopic examination (OLYMPUS
169 IX70, USA) according to Phytoplankton Manual (Sournia, 1978).

170

171 3. Results and Discussion

172 3.1. Dynamics of microalgae population

173 *Chlorella* sp., the inoculated microalgae species in R1, was detected throughout most of
174 the experimental period in this photobioreactor and dominant at days 37 and 86 (at
175 concentrations of $0.5 \cdot 10^9$ and $0.9 \cdot 10^9$ cells/L, respectively). *Acutodesmus obliquus* was
176 also identified in R1 and became the dominant species by day 58. Finally, *Aphanothece*
177 sp. was detected for the first time by day 58 and was dominant from day 122 to the end
178 of the operation of R1 (Figure 2a). Similarly, the inoculated microalga species in R2
179 (*Acutodesmus obliquus*) was identified along the entire photobioreactor operation, with
180 a significant dominance by days 37, 58 and 122 at cell concentrations of $1.3 \cdot 10^9$,
181 $1.8 \cdot 10^9$ and $0.3 \cdot 10^9$ cells/L, respectively. *Chlorella* sp. was identified in R2 from the
182 first operational days and remained at similar cell concentrations throughout the entire
183 experiment (from $0.3 \cdot 10^9$ to $0.7 \cdot 10^9$ cells/L). Finally, *Aphanothece* sp. became
184 dominant in R2 by the end of operation, with final cell concentrations of $2.9 \cdot 10^9$ cells/L
185 (Figure 2b). *Oscillatoria* sp. was replaced by *Chlorella* sp. and *Acutodesmus obliquus* in
186 R3 from the first operational days (after the inoculation a change in color from green to
187 red was noticed), *Chlorella* sp. being the dominant species throughout the entire
188 operation with a maximum concentration of $8.2 \cdot 10^9$ cells/L by day 58 (Figure 2c). The
189 higher pollution-tolerance of *Chlorella* sp. to PWW, combined with the high
190 temperature and irradiations prevailing in this study, could have caused this rapid
191 replacement of *Oscillatoria* sp (Talbot et al., 1991). Despite R4 was not inoculated,
192 *Chlorella* sp. and *Aphanothece* sp. were present in the photobioreactor from the first
193 days, *Chlorella* sp. being the dominant species along the 6 months of experiment. The

194 gradual increase in number of cells of *Aphanothece* sp. in R1, R2 and R4 suggest the
195 influence of the characteristics of the PWW on microalgae population (Figure 2).
196
197 The higher dominance of *Chlorella* sp. in the four photobioreactors confirmed the high
198 tolerance of this green microalgae to the pollutants and concentrations typically present
199 in PWW (Kim et al., 2016; Kuo et al., 2015; Yuan et al., 2013). Indeed, the high
200 abundance of *Acutodesmus obliquus* and *Chlorella* sp. (both belonging to the
201 Chlorophyta phylum) along the experimental period in R1, R2 and R3 matched the
202 microalgae pollution-tolerance classification reported by Palmer et al. (1969), who
203 ranked *Scenedesmus* and *Chlorella* 4th and 5th, respectively. It can be hypothesized that
204 organic pollution exhibited a higher influence on microalgae population structure than
205 other environmental parameters such as water hardness, light intensity, pH, DO or
206 temperature (Palmer, 1969). On the other hand, *Aphanothece* sp., which was not
207 previously classified as a pollution tolerant microalga, was mainly identified at the end
208 of experiment in R1 and R2 (Palmer, 1969). However, *Aphanothece microscopica*
209 *nägeli* and *Aphanothece Clathrata* successfully supported the removal of organic matter
210 and nitrogen from parboiled rice wastewater (REs of 83.4 and 72.7% for COD and N-
211 TKN, respectively) in a 4.5 L tubular photobioreactor operated batchwise for 24 hours
212 (Queiroz et al., 2007). Likewise, Bastos et al. (2014) reported COD and N-TKN REs of
213 97 and 78%, respectively, in a 4L batch tubular reactor treating parboiled rice
214 wastewater for 24 hours.

215

216 The lack of monoalgal cultures in the four photobioreactors throughout the
217 experimental period and the rapid variations in microalgae population structure here
218 recorded (mainly in R1 and R2) revealed the difficulty to maintain monoalgal cultures

219 during the treatment of PWW in open systems (Posadas et al., 2015). In this context, a
220 lower microalgae diversity was observed at higher biomass concentrations, which was
221 in agreement with Park et al. (2011). In addition, the current morphological microalgae
222 characterization revealed that the inoculation of a photobioreactor during PWW
223 treatment with a specific microalga does not guarantee its long-term dominance (Serejo
224 et al., 2015). Finally, it should be stressed that the different microalgae cells
225 concentration in the inoculum of the photobioreactors (1.750 , 0.295 and $0.332 \cdot 10^9$
226 cells/L for R1, R2 and R3, respectively) only affected the time required to reach steady
227 state and the initial treatment performance, but it did not modify the conclusions here
228 obtained since the performance of the systems was analyzed at constant under steady
229 state.

230

231 < Figure 2 >

232

233 **3.2. Biomass concentration and productivity**

234 Biomass concentration in R1, R2 and R3 increased from 220 mg TSS/L to 530, 680,
235 and 660 mg TSS/L, respectively, during the first 38 days. A moderate increase from 0 to
236 200 mg TSS/L was also recorded in R4 (Figure 3). A significant biomass concentration
237 increase occurred in R1, R2 and R3 from the day 38 to 93, when TSS concentrations of
238 2440, 2140 and 2500 mg TSS/L, respectively, were measured. However, a lower
239 biomass growth rate was observed during this period in R4, where concentrations up to
240 1200 mg TSS/L were recorded (Figure 3). Biomass concentration in R2 and R3
241 remained constant from day 93 onwards at average concentrations of 2569 ± 69 and
242 2445 ± 222 mg TSS/L, respectively. Biomass concentration in R1 fluctuated from day 93
243 to 150, to finally stabilize at 2610 ± 191 mg TSS/L, which was similar to the

244 concentrations reached in R2 and R3 (Figure 3). On the other hand, biomass
245 concentration exponentially increased in R4 from day 93, to reach average value of
246 3265 ± 133 mg TSS/L by the end of the experiment. Surprisingly, the highest algal-
247 bacterial biomass concentration under steady state was achieved in the non-inoculated
248 photobioreactor despite its longer lag phase. Likewise, the highest TOC, IC, TN, TP and
249 Zn REs (below discussed) were obtained in R4, which highlighted the higher robustness
250 of native microalgae species acclimated to the environmental and operational conditions
251 prevailing during PWW treatment (Figures 2 and 3, Table 1) (Olguín et al., 2013). In
252 addition, the results clearly showed a similar biomass growth pattern in the
253 photobioreactors inoculated with a specific photosynthetic microorganisms in
254 comparison with the control unit R4.

255

256 The high biomass concentrations here recorded were supported by the high carbon and
257 nutrients concentrations in the diluted PWW and by the high water evaporation rates in
258 the systems, which accounted for 60 % of the influent PWW in all photobioreactors as
259 noticed by Guieysse et al. (2013) (Table 1). Hence, biomass productivities under steady
260 state averaged 6.2 ± 0.5 , 6.1 ± 0.2 , 5.8 ± 0.6 and 7.8 ± 0.3 $\text{g/m}^2 \cdot \text{d}$ in R1, R2, R3 and R4,
261 respectively. These productivities were comparable to those obtained during the
262 treatment of secondary domestic wastewater treatment in pilot raceways at high HRT in
263 Almeria (Spain), and were likely limited by the long HRT needed to ensure satisfactory
264 organic matter and nutrients removals (Posadas et al., 2015).

265

266 Finally, the comparison between the evolution of the total number of microalgae cells in
267 the cultures and the TSS concentrations (Figures 2 and 3) showed no direct correlation
268 as a result of the dominant role of bacteria in the process, which itself was influenced by

269 the high biodegradable organic matter load. In this regard, an accurate empirical
270 determination of the individual bacteria and microalgae populations would bring
271 valuable insights about the mechanisms underlying organic matter and nutrient removal
272 during PWW treatment.

273

274 < Figure 3 >

275

276 **3.3 Carbon and nutrient removal**

277 A comparable bioremediation performance in terms of TOC, IC, TN and TP removal
278 was recorded regardless of the microalgae inoculated in the photobioreactor (Figure 4
279 and Table 1). In this context, the dominant microalgae species prevailing in the
280 photobioreactor did not influence process performance. In this particular study, the high
281 light irradiances and the optimum temperature for microbial activity supported an
282 effective PWW treatment. Thus, despite the low DO concentrations in the cultivation
283 broth (≤ 1.3 mg/L), TOC-REs accounted for 86 ± 1 , 87 ± 5 , 86 ± 1 and 86 ± 1 % in R1, R2,
284 R3 and R4, respectively, which resulted in average TOC concentrations in the effluent
285 at the end of the operational period of 459 ± 31 , 452 ± 31 , 482 ± 27 and 490 ± 37 mg/L,
286 respectively (Figure 4 and Table 1). Please note that the high water evaporation rates
287 typically encountered in open photobioreactors resulted in moderately high effluent
288 TOC concentration despite the high removal efficiencies achieved. The results herein
289 obtained confirmed the consistent removal of organic matter from PWW by algal-
290 bacterial processes and were in agreement with the study conducted by De Godos et al.
291 (2009), who reported COD removal efficiencies of 76 ± 11 % in a 464 L high rate algal
292 ponds (HRAP) during the treatment of 20 and 10 folds diluted PWW. Similarly, IC-REs
293 of 63 ± 3 , 69 ± 4 , 71 ± 4 and 62 ± 3 % were recorded at the end of the process in R1, R2, R3

294 and R4, respectively, which resulted in IC concentrations in the cultivation broth of the
295 photobioreactors of 285 ± 14 , 242 ± 34 , 227 ± 33 and 294 ± 27 mg/L, respectively (Figure 4
296 and Table 1). These high IC-REs were promoted by the intensive photosynthetic
297 activity during the illuminated period over the 176 days of operation. However, carbon
298 removal by stripping (prior mineralization of the organic carbon to CO_2) was the main
299 mechanism accounting for carbon fate, since only 37, 38, 36 and 48 % of the total
300 carbon removed was recovered in the harvested biomass in R1, R2, R3 and R4,
301 respectively, under steady state conditions. This estimation was based on the carbon
302 content of the biomass under steady state (as described below) and did not account for
303 the CO_2 input for pH control.

304

305 TN-REs of 82 ± 1 , 83 ± 3 , 83 ± 1 and 85 ± 1 % were recorded under steady state in R1, R2,
306 R3 and R4, respectively, which resulted in TN concentrations in the photobioreactor
307 effluent of 174 ± 11 , 166 ± 15 , 165 ± 12 and 149 ± 10 mg/L, respectively (Figure 4 and
308 Table 1). These high TN effluent concentrations in spite of the effective nitrogen
309 removal efficiencies were due to the high evaporation rates in the photobioreactors. The
310 TN-REs here recorded were similar to those reported by De Godos et al. (2009), who
311 measured average total kjeldahl nitrogen (TKN) removals of $86\pm 6\%$ during PWW
312 treatment in an open HRAP, and higher than the TN-REs of 63% obtained during the
313 treatment of PWW under laboratory conditions in a 500 ml conical flasks incubated on
314 a rotatory shaker at 27°C and 150 rpm under continuous illumination (Abou-Shanab et
315 al., 2013). Likewise, Posadas et al., (2017) operated an outdoors HRAP supporting TN-
316 REs of 80-86% during the treatment of centrate. Nitrogen removal by stripping was the
317 main mechanism in our study, since only 26, 26, 23 and 31 % of the total nitrogen
318 removed was recovered in the harvested biomass in R1, R2, R3 and R4, respectively.

319

320 On the other hand, steady state TP-REs of 90 ± 2 , 91 ± 1 , 92 ± 2 and 92 ± 2 % were
321 recorded in R1, R2, R3 and R4, respectively, which supported effluent TP
322 concentrations of 2.4 ± 0.3 , 2.1 ± 0.2 , 1.9 ± 0.5 and 1.8 ± 0.3 mg/L, respectively (Figure 4,
323 Table1). The TP-REs as ($P-PO_4^{3-}$) herein obtained were similar to those reported by
324 Posadas et al., (2017) during the treatment of centrate in an outdoors HRAP (84 - 92%).
325 Likewise, the TP-REs reported were in agreement with Franchino et al. (2016), who
326 recorded phosphate REs $> 90\%$ during the treatment of 5 and 10 times diluted digestate
327 in 250 ml flasks. Phosphorous assimilation into algal-bacterial biomass was the main
328 removal mechanism in the photobioreactors based on the moderate pH values prevailing
329 in the photobioreactors during the entire experiment (pH=8), which did not support a
330 significant phosphate precipitation (García et al., 2017). Thus, a phosphorus mass
331 balance revealed that 93, 93, 96 and 100 % of the total phosphorus removed was
332 recovered in the harvested biomass for R1, R2, R3 and R4, respectively.
333 Overall, it is worth noting that a similar macroscopic bioremediation performance was
334 recorded in the photobioreactors in spite of the different microalgae population
335 structures under steady state (and during most of the experiment period), which suggest
336 that bacteria played a dominant role during the treatment of high strength wastewaters
337 such as piggery effluents.

338

339

< Figure 4 >

340

341 Finally, comparable carbon, nitrogen and phosphorus contents were measured in the
342 harvested biomass under steady state regardless of the initial inoculum, with average
343 values of 50 ± 1 , 7.8 ± 0.3 and 0.75 ± 0.06 % for C, N and P, respectively (Figure 5). These

344 elemental biomass compositions were similar to those reported by Posadas et al. (2013)
345 during domestic wastewater treatment in a 15 L algal-bacterial biofilm photobioreactor
346 (42 ± 2 , 7 ± 1 and 1.3 ± 0.3 % for C, N and P, respectively), despite the different C/N/P
347 ratio in both wastewaters (C/N/P of 100/15.6/0.6 in PWW and 100/18/5 in domestic
348 wastewater). Likewise, these results were in agreement with those obtained by
349 Cabanelas et al. (2013), who reported a C, N and P content in the harvested biomass of
350 ≈ 44 , 7.5 and 0.5 %, respectively, in a photobioreactor inoculated with *Chlorella*
351 *vulgaris* and supplemented with CO₂ during the treatment of effluent from primary
352 settler. In this context, the results herein obtained confirmed the similar algal-bacterial
353 biomass composition regardless of the microalgae species present in the cultivation
354 broth or operational conditions.

355

356 < Figure 5 >

357

358 **3.4. Heavy metals removal efficiency**

359 The overall steady state Zn-REs in R1, R2, R3 and R4 accounted for 49 ± 6 , 37 ± 6 , 26 ± 5
360 and 49 ± 5 %, respectively, which resulted in average effluent Zn concentrations of
361 0.9 ± 0.2 , 1.1 ± 0.1 , 1.3 ± 0.3 and 0.9 ± 0.3 mg/L, respectively, at the end of the operational
362 period (Table 1). These values were similar (Zn-REs of 37%) to those reported by Abe
363 et al. (2008) during PWW treatment in wetlands. The fact that the highest Zn-REs
364 occurred in the photobioreactors with the highest biomass concentrations (R1 and R4)
365 and the lowest Zn-RE in R3 (at the lowest biomass concentration) suggested that Zn
366 removal was mediated by biosorption onto the algal-bacterial biomass present in the
367 photobioreactor (Table 1) (Kaplan et al., 1987; Muñoz et al., 2006). This showed the
368 high tolerance of species such as *Chlorella* sp. to heavy metal contamination (Muñoz et

369 al., 2006). Higher Zn-REs by biosorption would be expected at higher pHs according
370 to Muñoz et al. (2006), who observed an increase in Zn accumulation into the algal-
371 bacterial biomass from 5.0 to 11.7 mg Zn/g biomass when pHs was raised from 7 to 9,
372 respectively. The determination of copper and arsenic removal efficiencies was not
373 possible based on the low concentrations of these metals in the PWW (below the
374 detection limit of the instrument = 0.6 mg/L).

375

376 **4. Conclusions**

377 This research revealed the difficulty to maintain monoalgal cultures during PWW
378 treatment in open-photobioreactors operated under similar environmental and
379 operational conditions. The high abundance of *Chlorella* sp. in most photobioreactors
380 confirmed the high tolerance of this microalga to the pollutants. The acclimation of
381 native species to the characteristics of the PWW resulted in highest biomass
382 concentrations. An efficient PWW treatment occurred regardless of the microalgae
383 species inoculated, which confirmed the robustness of algal-bacterial processes devoted
384 to carbon and nutrient removals from livestock wastewaters. Finally, the heavy metals
385 can be removed by biosorption into the algal-bacterial biomass produced during PWW
386 bioremediation.

387

388 **5. Acknowledgments**

389 This research was supported by INIA, the European FEDER program (RTA2013-
390 00056-C03-02), the Regional Government of Castilla y León (Project VA024U14 and
391 UIC 71) and MINECO (Red Novedar). The financial support of the EU program

392 ERASMUS MUNDUS EURICA and Universidad Nacional Autónoma de Nicaragua
393 (UNAN-Managua) are also gratefully acknowledged.

394

395 **References**

- 396 1. Abe, K., Waki, M., Suzuki, K., Kasuya, M., Suzuki, R., Itahashi, S., Banzai, K.,
397 2012. Estimation of Zn and Cu unit output loads from animal husbandry facilities.
398 *Water Sci. Technol.* 66, 653–658. doi:10.2166/wst.2012.224
- 399 2. Abou-Shanab, R.A.I., Ji, M.-K., Kim, H.-C., Paeng, K.-J., Jeon, B.-H., 2013.
400 Microalgal species growing on piggery wastewater as a valuable candidate for nutrient
401 removal and biodiesel production. *J. Environ. Manage.* 115, 257–264.
402 doi:10.1016/j.jenvman.2012.11.022
- 403 3. Acién, F.G., Gómez-Serrano, C., Morales-Amaral, M.M., Fernández-Sevilla,
404 J.M., Molina-Grima, E., 2016. Wastewater treatment using microalgae: how realistic a
405 contribution might it be to significant urban wastewater treatment? *Appl. Microbiol.*
406 *Biotechnol.* 100, 9013–9022. doi:10.1007/s00253-016-7835-7
- 407 4. APHA, 2005. *Standards Methods for the Examination of Water and Wastewater*,
408 21 st. ed. American Public Health Association, American Water Works Association,
409 Water Environment Federation, Washington, D.C.
- 410 5. Bastos, R.G., Bonini, M. a., Zepka, L.Q., Jacob-Lopes, E., Queiroz, M.I., 2014.
411 Treatment of rice parboiling wastewater by cyanobacterium *Aphanothece microscopica*
412 *Nägeli* with potential for biomass products. *Desalin. Water Treat.* 3994, 1–7.
413 doi:10.1080/19443994.2014.937758
- 414 6. Cabanelas, I.T.D., Ruiz, J., Arbib, Z., Chinalia, F.A., Garrido-Pérez, C., Rogalla,
415 F., Nascimento, I.A., Perales, J.A., 2013. Comparing the use of different domestic
416 wastewaters for coupling microalgal production and nutrient removal. *Bioresour.*

417 Technol. 131, 429–436. doi:10.1016/j.biortech.2012.12.152

418 7. Chandrasekhar, K., Lee, Y.-J., Lee, D.-W., 2015. Biohydrogen Production:
419 Strategies to Improve Process Efficiency through Microbial Routes. *Int. J. Mol. Sci. Int.*
420 *J. Mol. Sci* 16, 8266–8293. doi:10.3390/ijms16048266

421 8. Cheah, W.Y., Ling, T.C., Show, P.L., Juan, J.C., Chang, J.S., Lee, D.J., 2016.
422 Cultivation in wastewaters for energy: A microalgae platform. *Appl. Energy* 179, 609–
423 625. doi:10.1016/j.apenergy.2016.07.015

424 9. De Godos, I., Blanco, S., García-Encina, P.A., Becares, E., Muñoz, R., 2009.
425 Long-term operation of high rate algal ponds for the bioremediation of piggery
426 wastewaters at high loading rates. *Bioresour. Technol.* 100, 4332–4339.
427 doi:10.1016/j.biortech.2009.04.016

428 10. De la Torre, A.I., Jiménez, J.A., Carballo, M., Fernandez, C., Roset, J., Muñoz,
429 M.J., 2000. Ecotoxicological evaluation of pig slurry. *Chemosphere* 41, 1629–1635.
430 doi:10.1016/S0045-6535(00)00038-2

431 11. Ehimen, E.A., Sun, Z.F., Carrington, C.G., Birch, E.J., Eaton-Rye, J.J., 2011.
432 Anaerobic digestion of microalgae residues resulting from the biodiesel production
433 process. *Appl. Energy* 88, 3454–3463. doi:10.1016/j.apenergy.2010.10.020

434 12. EU, 2016. https://ec.europa.eu/info/legal-notice_en [WWW Document]. URL
435 http://appsso.eurostat.ec.europa.eu/nui/show.do?dataset=apro_mt_lspig&lang=en
436 (accessed 11.7.16).

437 13. EU, 2015. <http://ec.europa.eu> [WWW Document]. URL
438 [http://ec.europa.eu/eurostat/statistics-explained/index.php/Agricultural_production_-](http://ec.europa.eu/eurostat/statistics-explained/index.php/Agricultural_production_-_animals)
439 [_animals](http://ec.europa.eu/eurostat/statistics-explained/index.php/Agricultural_production_-_animals) (accessed 1.10.17).

440 14. Franchino, M., Tigini, V., Varese, G.C., Mussat Sartor, R., Bona, F., 2016.
441 Microalgae treatment removes nutrients and reduces ecotoxicity of diluted piggery

- 442 digestate. *Sci. Total Environ.* 569, 40–45. doi:10.1016/j.scitotenv.2016.06.100
- 443 15. García, D., Alcántara, C., Blanco, S., Pérez, R., Bolado, S., Muñoz, R., 2017.
- 444 Enhanced carbon, nitrogen and phosphorus removal from domestic wastewater in a
- 445 novel anoxic-aerobic photobioreactor coupled with biogas upgrading. *Chem. Eng. J.*
- 446 313, 424–434. doi:10.1016/j.cej.2016.12.054
- 447 16. González-Fernández, C., Sialve, B., Bernet, N., Steyer, J., 2012a. Impact of
- 448 microalgae characteristic on their conversion to biofuel. Part I: Focus on cultivation and
- 449 biofuel production. *Biofuels, Bioprod. Biorefining* 105–113. doi:10.1002/bbb
- 450 17. González-Fernández, C., Sialve, B., Bernet, N., Steyer, J., 2012b. Impact of
- 451 microalgae characteristics on their conversion to biofuel. Part II: Focus on biomethane
- 452 production. *Biofuels, Bioprod. Biorefining* 205–218. doi:10.1002/bbb
- 453 18. Guieysse, B., Béchet, Q., Shilton, A., 2013. Variability and uncertainty in water
- 454 demand and water footprint assessments of fresh algae cultivation based on case studies
- 455 from five climatic regions. *Bioresour. Technol.* 128, 317–323.
- 456 doi:10.1016/j.biortech.2012.10.096
- 457 19. Kaplan, D., Cristiaen, D., Shoshana, A., 1987. Chelating Properties of
- 458 Extracellular Polysaccharides from *Chlorella* spp. *Appl. Environ. Microbiol.* 53, 2953–
- 459 2956.
- 460 20. Kim, H.-C., Choi, W.J., Chae, A.N., Park, J., Kim, H.J., Song, K.G., 2016.
- 461 Treating high-strength saline piggery wastewater using the heterotrophic cultivation of
- 462 *Acutodesmus obliquus*. *Biochem. Eng. J.* 110, 51–58. doi:10.1016/j.bej.2016.02.011
- 463 21. Kuo, C.M., Chen, T.Y., Lin, T.H., Kao, C.Y., Lai, J.T., Chang, J.S., Lin, C.S.,
- 464 2015. Cultivation of *Chlorella* sp. GD using piggery wastewater for biomass and lipid
- 465 production. *Bioresour. Technol.* 194, 326–333. doi:10.1016/j.biortech.2015.07.026
- 466 22. MAGRAMA, 2015. Censo y producción: Producción de porcino ibérico [WWW

- 467 Document]. URL [http://www.magrama.gob.es/es/ganaderia/temas/produccion-y-](http://www.magrama.gob.es/es/ganaderia/temas/produccion-y-mercados-ganaderos/sectores-ganaderos/porcino/)
468 [mercados-ganaderos/sectores-ganaderos/porcino/](http://www.magrama.gob.es/es/ganaderia/temas/produccion-y-mercados-ganaderos/sectores-ganaderos/porcino/) (accessed 10.18.16).
- 469 23. Muñoz, R., Alvarez, M.T., Muñoz, A., Terrazas, E., Guieysse, B., Mattiasson,
470 B., 2006. Sequential removal of heavy metals ions and organic pollutants using an
471 algal-bacterial consortium. *Chemosphere* 63, 903–11.
472 doi:10.1016/j.chemosphere.2005.09.062
- 473 24. Muñoz, R., Guieysse, B., 2006. Algal-bacterial processes for the treatment of
474 hazardous contaminants: A review. *Water Res.* 40, 2799–2815.
475 doi:10.1016/j.watres.2006.06.011
- 476 25. Muñoz, R., Köllner, C., Guieysse, B., Mattiasson, B., 2003. Salicylate
477 biodegradation by various algal-bacterial consortia under photosynthetic oxygenation.
478 *Biotechnol. Lett.* 25, 1905–1911. doi:10.1023/B:BILE.0000003980.96235.fd
- 479 26. Naik, S.N., Goud, V. V., Rout, P.K., Dalai, A.K., 2010. Production of first and
480 second generation biofuels: A comprehensive review. *Renew. Sustain. Energy Rev.* 14,
481 578–597. doi:10.1016/j.rser.2009.10.003
- 482 27. Olguín, E.J., Mendoza, A., González-Portela, R.E., Novelo, E., 2013. Population
483 dynamics in mixed cultures of *Neochloris oleoabundans* and native microalgae from
484 water of a polluted river and isolation of a diatom consortium for the production of lipid
485 rich biomass. *N. Biotechnol.* 30, 705–715. doi:10.1016/j.nbt.2013.03.003
- 486 28. Palmer, C.M., 1969. A composite rating of algae tolerating organic pollution. *J.*
487 *Phycol.* 5, 78–82. doi:10.1111/j.1529-8817.1969.tb02581.x
- 488 29. Park, J.B.K., Craggs, R.J., Shilton, A.N., 2011. Recycling algae to improve
489 species control and harvest efficiency from a high rate algal pond. *Water Res.* 45, 6637–
490 6649. doi:10.1016/j.watres.2011.09.042
- 491 30. Posadas, E., García-Encina, P.A., Soltau, A., Domínguez, A., Díaz, I., Muñoz,

- 492 R., 2013. Carbon and nutrient removal from centrates and domestic wastewater using
493 algal-bacterial biofilm bioreactors. *Bioresour. Technol.* 139, 50–58.
494 doi:10.1016/j.biortech.2013.04.008
- 495 31. Posadas, E., Marín, D., Blanco, S., Lebrero, R., Muñoz, R., 2017. Simultaneous
496 biogas upgrading and centrate treatment in an outdoors pilot scale high rate algal pond.
497 *Bioresour. Technol.* doi:10.1016/j.biortech.2017.01.071
- 498 32. Posadas, E., Morales, M.D.M., Gomez, C., Ación, F.G., Muñoz, R., 2015.
499 Influence of pH and CO₂ source on the performance of microalgae-based secondary
500 domestic wastewater treatment in outdoors pilot raceways. *Chem. Eng. J.* 265, 239–248.
501 doi:10.1016/j.cej.2014.12.059
- 502 33. Posadas, E., Serejo, M.L., Blanco, S., Pérez, R., García-Encina, P.A., Muñoz, R.,
503 2015. Minimization of biomethane oxygen concentration during biogas upgrading in
504 algal-bacterial photobioreactors. *Algal Res.* 12, 221–229.
505 doi:10.1016/j.algal.2015.09.002
- 506 34. Queiroz, M.I., Lopes, E.J., Zepka, L.Q., Bastos, R.G., Goldbeck, R., 2007. The
507 kinetics of the removal of nitrogen and organic matter from parboiled rice effluent by
508 cyanobacteria in a stirred batch reactor. *Bioresour. Technol.* 98, 2163–2169.
509 doi:10.1016/j.biortech.2006.08.034
- 510 35. Richmond, A., 2004. *Handbook of microalgal culture: biotechnology and*
511 *applied phycology*/edited by Amos Richmond. doi:10.1002/9780470995280
- 512 36. Serejo, M.L., Posadas, E., Boncz, M.A., Blanco, S., García-Encina, P., Muñoz,
513 R., 2015. Influence of Biogas Flow Rate on Biomass Composition During the
514 Optimization of Biogas Upgrading in Microalgal-Bacterial Processes. *Environ. Sci.*
515 *Technol.* 3228–3236. doi:10.1021/es5056116
- 516 37. Sournia, A., 1978. *Phytoplankton manual*. UNESCO, Paris.

- 517 38. Talbot, P., Thébault, J., Dauta, A., De la Noüe, J., 1991. A comparative study
518 and mathematical modeling of temperature, light and growth of three microalgae
519 potentially useful for wastewater treatment. *Water Res.* 25, 465–472. doi:10.1016/0043-
520 1354(91)90083-3
- 521 39. Vimalarasan, A., Pratheeba, N., Ashokkumar, B., Sivakumar, N., Varalakshmi,
522 P., 2011. Production of biodiesel from cyanobacteria (*Oscillatoria annae*) by alkali and
523 enzyme mediated transesterification. *J. Sci. Ind. Res. (India)*. 70, 959–967.
- 524 40. Yuan, Z., Wang, Z., Takala, J., Hiltunen, E., Qin, L., Xu, Z., Qin, X., Zhu, L.,
525 2013. Scale-up potential of cultivating *Chlorella zofingiensis* in piggery wastewater for
526 biodiesel production. *Bioresour. Technol.* 137, 318–325.
527 doi:10.1016/j.biortech.2013.03.144
528

529 **Figure captions**

530 **Figure 1.** Schematic diagram of the algal-bacterial photobioreactor set-up using carbon
531 dioxide supplementation for pH control.

532 **Figure 2.** Time course of microalgae population structure in (a) R1, (b) R2, (c) R3 and
533 (d) R4. *Acutodesmus obliquus* (▨), *Aphanothece* sp. (■), *Chlorella* sp. (▩), *Oscillatoria*
534 sp. (▧) and total number of microalgae cells (■).

535 **Figure 3.** Time course of TSS concentration in R1 (Δ), R2 (◇), R3 (□) and R4 (○).

536 **Figure 4.** Average removal efficiencies of TOC (▨), IC (▩), TN (■) and TP (▧)
537 under steady state. Vertical bars represent the standard deviation from replicate
538 measurements during steady state operation.

539 **Figure 5.** C (▨), N (▩), and P (■) content in the biomass present in the
540 photobioreactors under steady state.

Figure 1. Schematic diagram of the algal-bacterial photobioreactor set-up using carbon dioxide supplementation for pH control.

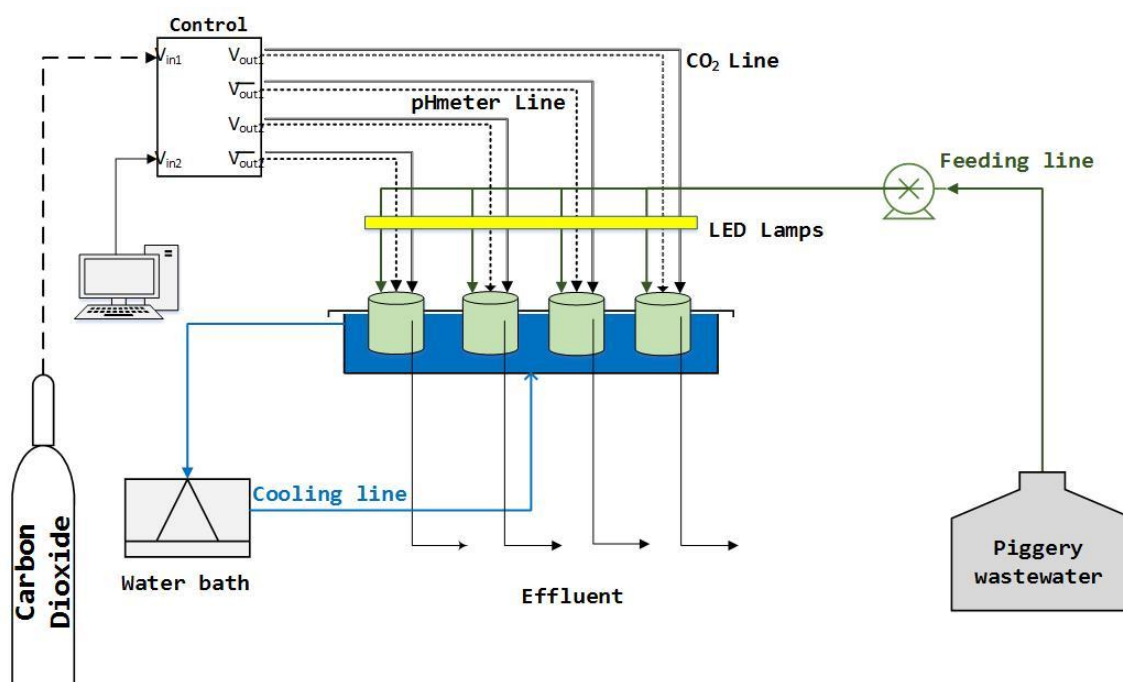


Figure 2. Time course of microalgae population structure in (a) R1, (b) R2, (c) R3 and (d) R4. *Acutodesmus obliquus* (▨), *Aphanothece* sp. (■), *Chlorella* sp. (▩), *Oscillatoria* sp. (▤) and total number of microalgae cells (●).

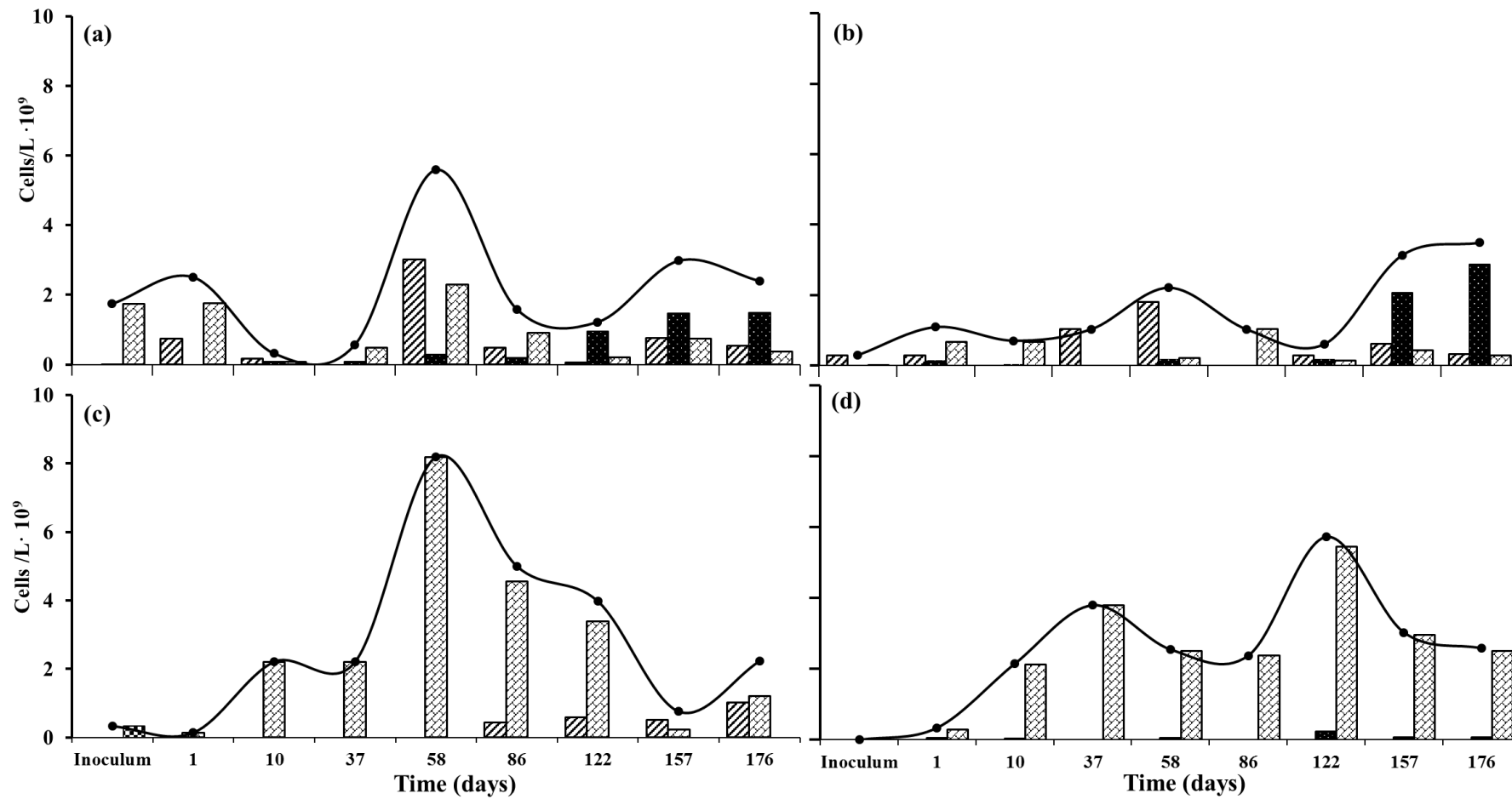


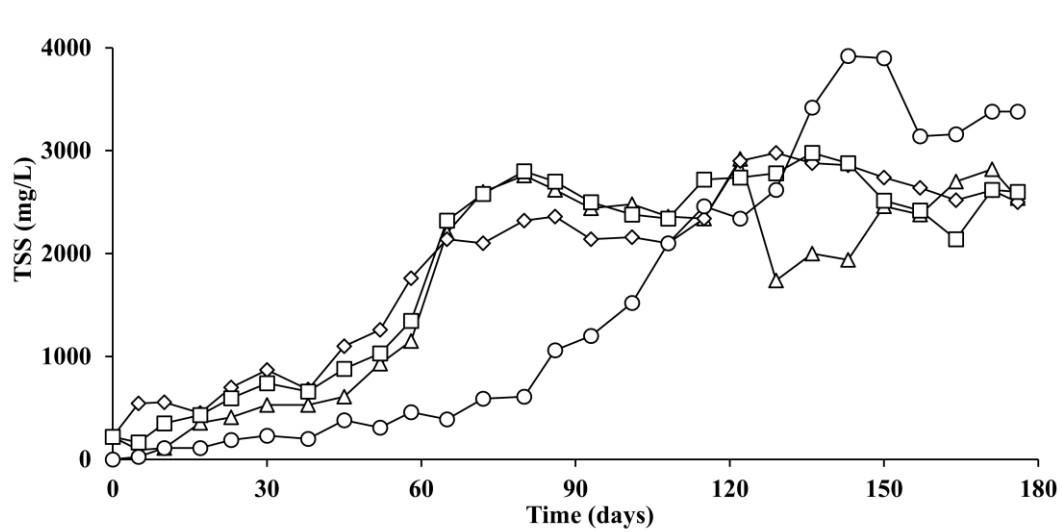
Figure 3. Time course of TSS concentration in R1 (Δ), R2 (\diamond), R3 (\square) and R4 (\circ).

Figure 4. Average removal efficiencies of TOC (□), IC (▨), TN (■) and TP (▩) under steady state. Vertical bars represent the standard deviation from replicate measurements during steady state operation.

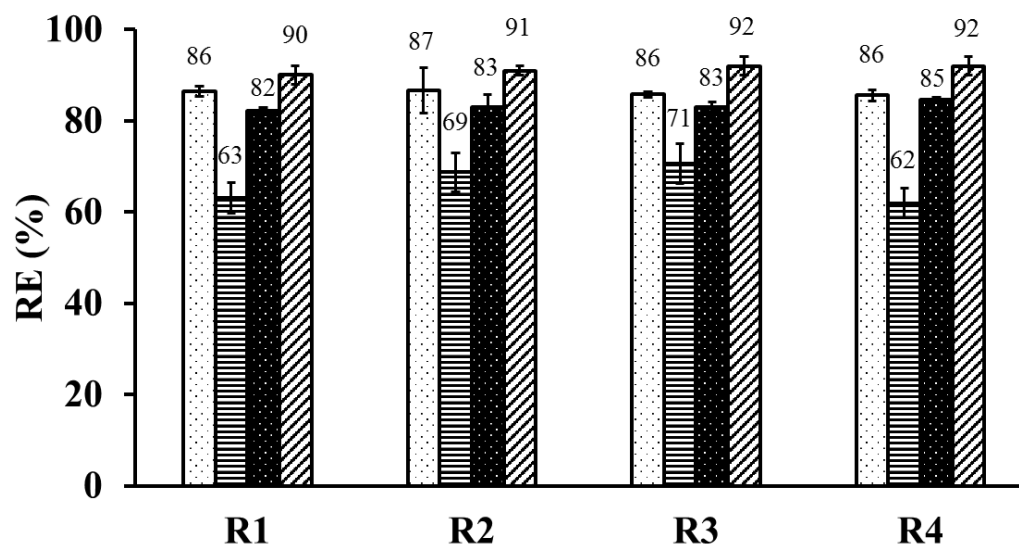


Figure 5. C (▨), N (▤) and P (■) content in the biomass present in the photobioreactors under steady state.

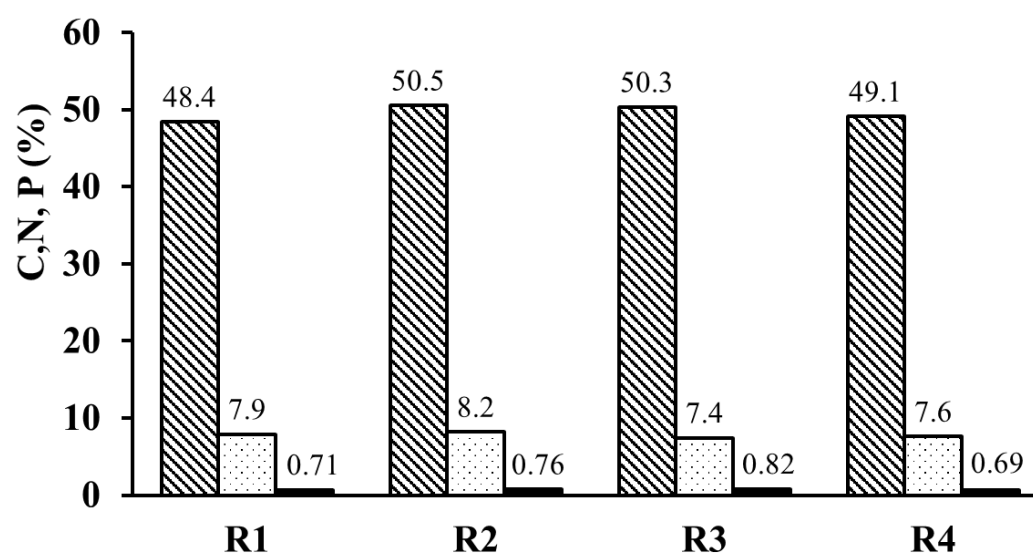


Table 1. Physical/chemical characterization of the diluted swine manure and cultivation broth in the photobioreactors at steady state.

Parameter	PWW	R1	R2	R3	R4
Evaporation (%)	n.a	60±6	60±7	60±6	60±8
Temperature (°C)	n.a	30±2	30±2	30±2	30±2
Dissolved Oxygen (mg/L)	n.a	0.8	1.1	1.3	0.9
TOC (mg/L)	1375±121	459±31	452±31	482±27	490±37
IC (mg/L)	314±55	285±14	242±34	227±33	294±27
TN (mg/L)	393±26	174±11	166±15	165±12	149±10
Nitrite (mg/L)	< 0.5	< 0.5	< 0.5	< 0.5	< 0.5
Nitrate (mg/L)	< 0.5	< 0.5	< 0.5	< 0.5	< 0.5
TP (mg/L)	9.4±0.4	2.4±0.3	2.1±0.2	1.9±0.5	1.8±0.3
Zinc (mg/L)	0.7±0.2	0.9±0.2	1.1±0.1	1.3±0.3	0.9±0.3
Copper (mg/L)	< 0.6	< 0.6	< 0.6	< 0.6	< 0.6
Arsenic (mg/L)	< 0.6	< 0.6	< 0.6	< 0.6	< 0.6
TSS (mg/L)	1340±34	2610±191	2569±69	2445±222	3265±133
n.a : Not applicable					

Electronic Annex

[Click here to download Electronic Annex: Supplementary materials_Garcia_BITE.docx](#)